A luminal flavoprotein in endoplasmic reticulum-associated degradation

Jan Riemer[a,b], Christian Appenzeller-Herzog[a], Linda Johansson[a], Bernd Bodenmiller[b,c], Rasmus Hartmann-Petersen[a], and Lars Ellgaard[a,1]

[a]Department of Biology, University of Copenhagen, 2200 Copenhagen, Denmark; [c]Department of Molecular Systems Biology, Eidgenössische Technische Hochschule, 8093 Zurich, Switzerland; and [b]PhD Program in Molecular Life Sciences, Life Science Zurich Graduate School, 8057 Zurich, Switzerland

Edited by Hidde L. Ploegh, Whitehead Institute for Biomedical Research, Cambridge, MA, and accepted by the Editorial Board June 30, 2009 (received for review January 22, 2009)

The quality control system of the endoplasmic reticulum (ER) discriminates between native and nonnative proteins. The latter are degraded by the ER-associated degradation (ERAD) pathway. Whereas many cytosolic and membrane components of this system are known, only few luminal players have been identified. In this study, we characterize ERFAD (ER flavoprotein associated with degradation), an ER luminal flavoprotein that functions in ERAD. Upon knockdown of ERFAD, the degradation of the ERAD model substrate ribophorin 332 is delayed, and the overall level of polyubiquitinated cellular proteins is decreased. We also identify the ERAD components SEL1L, OS-9 and ERdj5, a known reductase of ERAD substrates, as interaction partners of ERFAD. Our data show that ERFAD facilitates the dislocation of certain ERAD substrates to the cytosol, and we discuss the findings in relation to a potential redox function of the protein.

ERdj5 | OS-9 | SEL1L | ERFAD | ERAD

In the secretory pathway, critical protein maturation steps occur in the endoplasmic reticulum (ER). During translocation of the polypeptide chain into the ER, modifications such as N-glycosylation and disulfide-bond formation take place, and a variety of chaperones assist folding. Whereas native proteins can exit the ER by the secretory pathway, misfolded proteins and incompletely assembled protein complexes are retained by the quality control machinery of the ER (1). To prevent their toxic accumulation, nonnative proteins are degraded by the cytosolic ubiquitin-proteasome system. First, proteins must be recognized as nonnative. They are then transported to the site of retrotranslocation and extracted from the ER. Partial unfolding and/or reduction are likely prerequisites for transport across the membrane for many proteins. In the cytosol, proteins become polyubiquitinated by ubiquitin ligases before degradation by the proteasome. Collectively, the various steps of this process are known as ER-associated degradation (ERAD) (2, 3).

Different ERAD pathways have been defined (3). One of them is the Hrd-ligase pathway. In yeast and presumably in metazoans it mediates the degradation of proteins with luminal lesions (4). The central components of this pathway are two closely associated membrane proteins, the ubiquitin ligase Hrd1 (Hrd1p in yeast) and SEL1L (Hrd3p). SEL1L contains a large luminal domain (5–7) that likely serves as an adaptor platform for ERAD factors such as the chaperones BiP (Kar2p) and GRP94 as well as the lectin OS-9 (Yos9p) (5, 6, 8). These factors deliver misfolded proteins to SEL1L and thereby mediate the recognition of luminal substrates by the Hrd-ligase complex (9–12).

After the initial recognition step, disulfide bonds in ERAD substrates can be reduced by ERdj5 (13), a thiol-disulfide oxidoreductase of the protein disulfide isomerase (PDI) family, and luminal ERAD substrates traverse the ER membrane likely through a retrotranslocation channel (2). In the cytosol, all known ERAD pathways converge at the AAA-ATPase p97 (Cdc48p) that extracts substrates from the ER (14, 15). If substrates contain N-glycans, they are deglycosylated at this stage by the cytosolic peptidyl:N-glycanase (Png1) (16) before being degraded by the proteasome (17).

Here, we identify the ER luminal flavoprotein ERFAD that we show to interact with SEL1L, OS-9, and ERdj5. Moreover, down-regulation of ERFAD stabilizes the ERAD substrate RI_{332} and reduces the cellular level of polyubiquitinated proteins. Based on the data, and in light of the unique sequence features of ERFAD, we discuss possible mechanisms of action in ERAD.

Results and Discussion

ERFAD Is a Flavoprotein of the ER. To find redox-active ER proteins, we performed database searching for homologs of the cytosolic protein glutathione reductase (GR). This enzyme utilizes the two redox cofactors NADPH and FAD. During catalysis, two NADPH-derived electrons are transferred via FAD onto a pair of cysteines that then acts as a disulfide reductant. Performing a BLAST search with GR as query sequence we identified a previously uncharacterized ORF (RefSeq: NP 079231, gene name: FOXRED2) that encodes a protein of 684 amino acids. Unlike GR, the N-terminal 26 residues are predicted to constitute an ER signal peptide, and the protein contains a C-terminal "KEEL" ER-retrieval motif characteristic of soluble ER proteins (Fig. 1*A*). Based on this in silico analysis and on our functional studies (see below), we termed the protein ER flavoprotein associated with degradation (ERFAD). Whereas the C-terminal ≈250 residues of ERFAD do not contain any known domains, the N-terminal ≈400 residues of the protein comprise, like GR and the related thioredoxin reductase (TR), consensus motifs for the binding of the two redox cofactors FAD and NADPH (Fig. 1*A*). It is noteworthy that despite the homology to GR and TR, ERFAD does not contain an equivalent of the redox-active Cys-Xaa_4-Cys motif found in these two enzymes, making it unlikely that ERFAD functions by the same mechanism. Database searching revealed orthologs of ERFAD in a number of vertebrates, urochordates and in *S. purpuratus* (a sea urchin) and *O. tauri* (an algae), but not in the model organisms *S. cerevisiae*, *D. melanogaster*, and *C. elegans*. In silico and RT-PCR analysis showed a broad tissue distribution of human ERFAD transcripts (Fig. 1*B*).

To investigate whether ERFAD is indeed a flavoprotein, we purified ERFAD from a HEK293 cell line stably expressing the full-length protein containing C-terminal hexa-His and FLAG tags (3B2B cells) (Fig. 1*C*). Whereas in most preparations we detected only pure ERFAD, in others we copurified varying amounts of BiP. This suggested that a fraction of ERFAD-His-FLAG, which was heavily overexpressed in 3B2B cells (≈30 times compared with endogenous levels; Fig. S1*A*), required BiP binding to remain

Author contributions: J.R., C.A.-H., L.J., B.B., and L.E. designed research; J.R., C.A.-H., L.J., B.B., and R.H.-P. performed research; J.R., C.A.-H., L.J., B.B., R.H.-P., and L.E. analyzed data; and J.R. and L.E. wrote the paper.

The authors declare no conflict of interest.

This article is a PNAS Direct Submission. H.L.P. is a guest editor invited by the Editorial Board.

[1]To whom correspondence should be addressed. E-mail: lellgaard@bio.ku.dk.

This article contains supporting information online at www.pnas.org/cgi/content/full/0900742106/DCSupplemental.

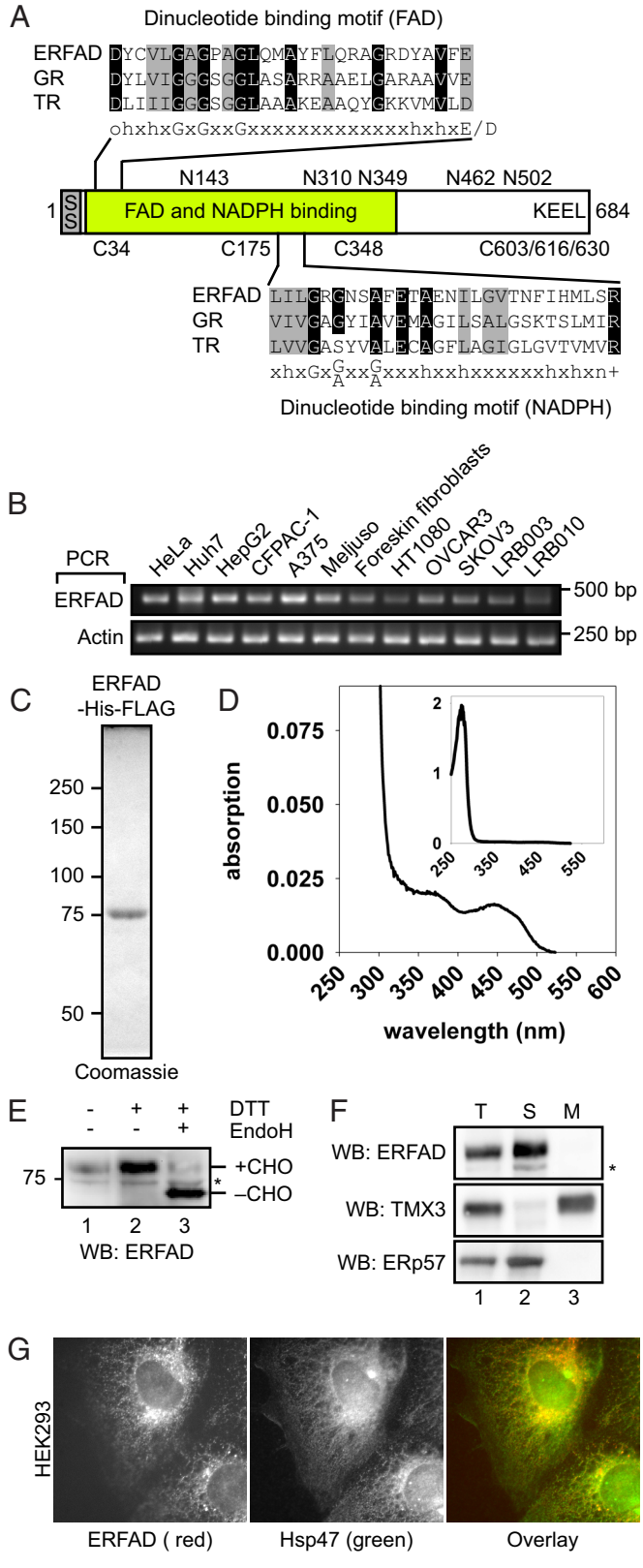

Fig. 1. ERFAD is an ER flavoprotein. (*A*) Domain organization of the ERFAD protein. The two dinucleotide-binding motifs of the GXGXXG-type for FAD and NADPH binding are shown aligned with the corresponding motifs in GR, TR, and a consensus motif (amino acid residues: h = hydrophobic, o = polar/charged, + = positively charged, *n* = neutral). The sequence positions of the five N-glycosylation sites and the six cysteines in ERFAD are depicted. SS, signal sequence. (*B*) RT-PCR analysis of ERFAD. Total RNA was isolated from different human tissue culture cells, reverse transcribed and amplified with primers specific for ERFAD and actin. HeLa: cervical epithelial carcinoma; Huh7, HepG2: hepatocellular carcinoma; CF-PAC-1: pancreatic adeno carcinoma; A375, Meljuso: melanoma; HT1080: fibrosarcoma breast cancer; OVCAR3, SKOV3: ovarian epithelial carcinoma; LRB003, LRB010: embryonic stem cells (*C*) Purified recombinant ERFAD-His-FLAG visualized by Coomassie staining. (*D*) Absorption spectra of purified ERFAD-His-FLAG. The two peaks at 370 nm and 450 nm are indicative of the flavin cofactor. (*Inset*) Complete spectrum including the protein peak at 280 nm. (*E*) Glycosylation and oxidation state of human ERFAD. Lysates from HEK293 cells were treated as indicated, and analyzed by Western blotting against endogenous ERFAD. *, background band; CHO, N-glycans. (*F*) Subcellular fractionation of HEK293 cells. After isolation and sodium carbonate extraction of crude membranes, followed by ultracentrifugation through a sucrose cushion, the distribution of ERFAD, ERp57 (a soluble ER protein) and TMX3 (an ER membrane protein) was visualized by Western blot analysis. *, background band. (*G*) Immunofluorescence microscopy of ERFAD in HEK293 cells. Cells were fixed and stained with anti-ERFAD (*Left*, 1F6, red) and anti-Hsp47 (*Center*, green). A merged image is shown in the *Right*.

soluble. In the absorption spectrum of purified ERFAD we detected two peaks with maxima at 370 and 450 nm characteristic of a flavin cofactor in addition to the protein peak at 280 nm (Fig. 1*D*). To assess the cofactor binding in more detail, we released the flavin with 0.1% SDS and separated it from the protein by filtration. In the filtrate, we observed a fluorescence emission peak at 535 nm upon excitation at 450 nm. Typical for free FAD (and not FMN) (18), this signal increased upon acidification of the solution to pH 3. Such a signal was not observed without prior denaturation of the protein indicating the specific binding of FAD to ERFAD.

To facilitate the analysis of endogenous ERFAD, we raised an antiserum against the denatured full-length protein. After affinity purification this antiserum recognized a band of ≈80 kDa corresponding to ERFAD (calculated molecular mass of 75.3 kDa without N-glycans) and a second weaker band at ≈75 kDa (Fig. 1 *E* and *F* and Fig. S1*B*). The latter band likely represents a protein unrelated to ERFAD because siRNA-mediated down-regulation of ERFAD reduced the intensity of the 80-kDa band only (Fig. S2 *A* and *C*). As expected for an ER protein with five potential N-glycosylation sites (Fig. 1*A*), increased mobility was observed upon EndoH cleavage (Fig. 1*E*). Nonreducing SDS/PAGE resulted in only a marginal shift of the ERFAD band, suggesting that none of the six cysteines in ERFAD (Fig. 1*A*) are enganged in long-range intramolecular disulfide bonds (Fig. 1*E*). Alkali extraction of crude membranes demonstrated that ERFAD is a soluble protein (Fig. 1*F*). In immunofluorescence microscopy, we observed a reticular staining pattern for ERFAD and colocalization with the ER chaperone Hsp47 (Fig. 1*G*). A similar result was obtained with transiently expressed HA-tagged ERFAD (Fig. S1*C*). We concluded that ERFAD is a ubiquitous soluble N-glycosylated ER flavoprotein.

ERFAD Interacts with the ERAD Components SEL1L, OS-9, and ERdj5. To provide clues for the cellular function of ERFAD, we set out to identify interaction partners. For this purpose, we generated a HEK293-derived cell line stably expressing the protein with an HA tag inserted immediately before the C-terminal KEEL sequence (A11 cells). Immunoprecipitation of ERFAD-HA with two different monoclonal HA antibodies (16B12 and 12CA5) revealed one clear candidate interacting protein (Fig. 2*A*, arrowheads). This protein had an apparent size of ≈90 kDa and contained EndoH-sensitive glycans (Fig. 2*B*). Scaling up of the coimmunoprecipitation experiment allowed protein identification by mass spectrometry on a glycosidase-treated sample. The results showed the excised band to contain the important ERAD component SEL1L.

To verify the interaction between ERFAD and SEL1L, we immunoprecipitated ERFAD-HA from A11 cells and analyzed the eluate by Western blotting using anti-SEL1L (Fig. 2*C*, lane 4). In another experiment, we immunoprecipitated SEL1L from A11 cells and blotted the eluted proteins with anti-HA (Fig. 2*D*, lane 4). In

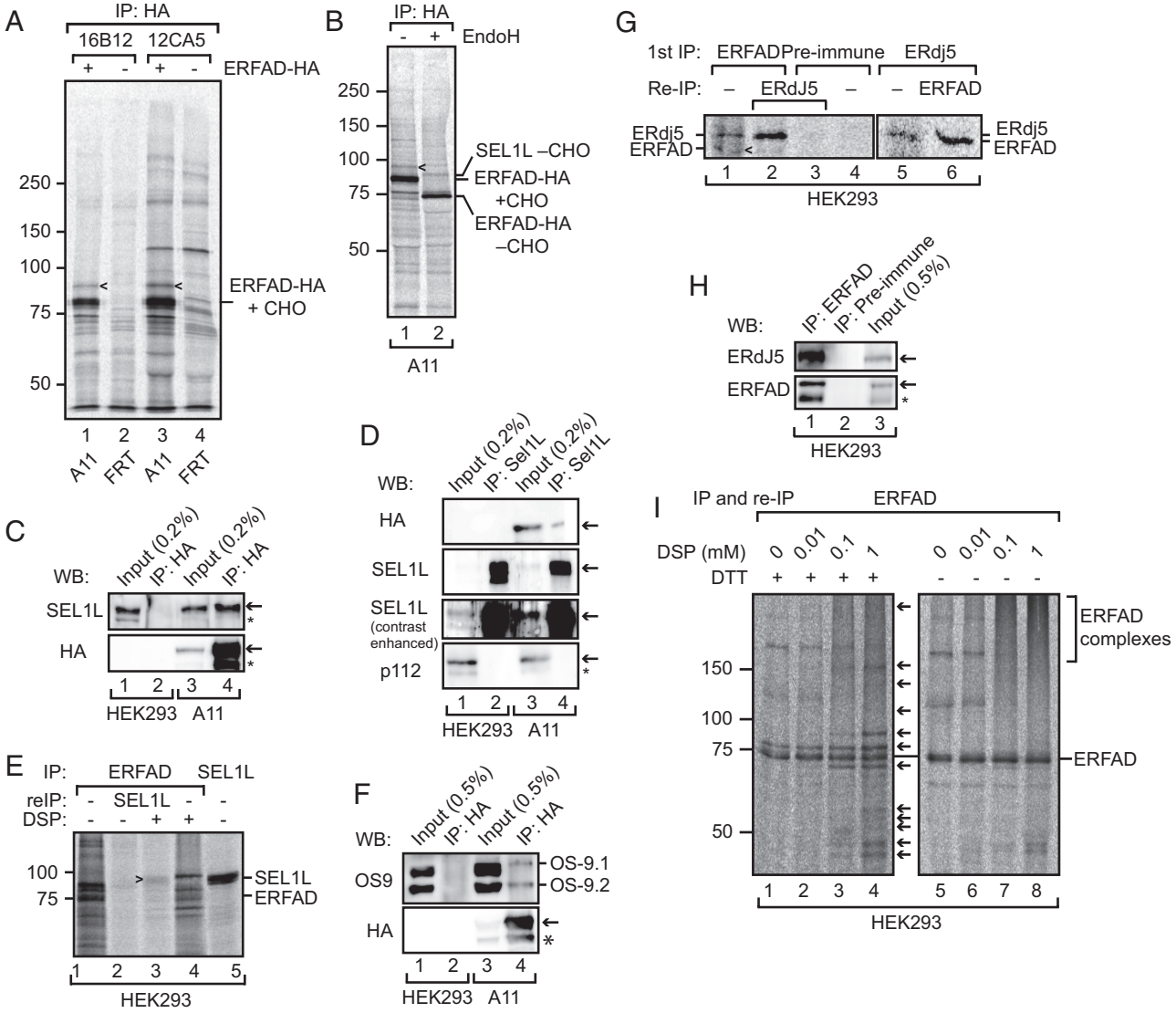

Fig. 2. ERFAD interacts with the ERAD components SEL1L, OS-9, and ERdj5. (*A*) Immunoprecipitation of ERFAD-HA. Cells stably expressing ERFAD-HA (A11) and control cells (FRT) were [^{35}S] pulse-labeled for 16 h, Triton X-100 lysates immunoprecipitated with anti-HA (16B12 and 12CA5), and samples separated by reducing SDS/PAGE. The position of a coimmunoprecipitating 90 kDa band is indicated by arrowheads. (*B*) Immunoprecipitation of ERFAD-HA with 16B12, undigested (lane 1) and digested (lane 2) with EndoH. The position of the protein identified by mass spectrometry—SEL1L—is indicated. CHO, N-glycans. (*C*) SEL1L coimmunoprecipitates with ERFAD-HA. Immunoprecipitations from lysates of A11 or HEK293 cells were performed with anti-HA, and subsequently analyzed by Western blotting as indicated. *, background band. (*D*) ERFAD-HA coimmunoprecipitates with SEL1L. Immunoprecipitations from lysates of A11 cells were performed with anti-SEL1L and subsequently analyzed by Western blotting with anti-HA, anti-SEL1L (contrast-enhanced blot included to better see the input), and anti-p112 as a specificity control. *, background band. (*E*) Endogenous ERFAD and SEL1L coimmunoprecipitate upon cross-linking with DSP. After incubation with DSP, ERFAD was immunoprecipitated from [^{35}S] pulse-labeled HEK293 cells. The immunoprecipitate was either analyzed directly (lanes 1 and 4) or reimmunoprecipitated with antibodies against SEL1L (lane 2 and 3). For comparison an anti-SEL1L immunoprecipitate is loaded in lane 5. Samples were analyzed by reducing SDS/PAGE, which resolves the thiol-cleavable cross-link between ERFAD and SEL1L. (*F*) OS-9.1 and 9.2 coprecipitate with ERFAD-HA. Immunoprecipitations from A11 or HEK293 cell lysates were performed with anti-HA, and analyzed by Western blotting with antibodies against OS-9 and the HA tag. *, background band. (*G*) Endogenous ERFAD and ERdj5 coimmunoprecipitate. ERFAD was immunoprecipitated from [^{35}S] pulse-labeled HEK293 cells with anti-ERFAD (SG2480). The immunoprecipitate was either analyzed directly (lane 1) or reimmunoprecipitated with anti-ERdj5 (lane 2). As a control, preimmune serum was used instead of anti-ERFAD (lanes 3 and 4). In another experiment, ERdj5 was immunoprecipitated from pulse-labeled HEK293 cells and either analyzed directly (lane 5) or immunoprecipitated with anti-ERFAD (lane 6). Samples were analyzed by reducing SDS/PAGE. Arrowhead, ERFAD. (*H*) Endogenous ERFAD and ERdj5 coimmunoprecipitate. Immunoprecipitations from lysates of HEK293 cells were performed with anti-ERFAD (1F6) or preimmune serum and subsequently analyzed by Western blotting with anti-ERdj5 and anti-ERFAD. *, background band. (*I*) Numerous proteins immunoprecipitate with endogenous ERFAD upon DSP cross-linking. Immunoprecipitates of ERFAD after treatment with increasing concentrations of DSP were either analyzed under reducing or nonreducing conditions. Arrows indicate proteins that coprecipitate with ERFAD upon cross-linking. For complete audiographs see Fig. S3 .

both cases, we observed an interaction between the two proteins. We could also detect the interaction between endogenous ERFAD and SEL1L when using the thiol-cleavable cross-linker dithiobis(succinimidyl)propionate (DSP) to stabilize the complex (Fig. 2*E*, lane 3). In addition to SEL1L, we found ERFAD to interact with two further ERAD proteins. First, the immunoprecipitate of ERFAD-HA from A11 cells contained both isoforms of OS-9 (Fig. 2*F*, lane 4). Second, the PDI-family member ERdj5 precipitated with endogenous ERFAD (Fig. 2*G*, lane 2, and *H*, lane 1), and ERFAD precipitated with endogenous ERdj5 (Fig. 2*G*, lane 6).

Interestingly, when using DSP we precipitated with ERFAD several additional proteins that were also recovered when

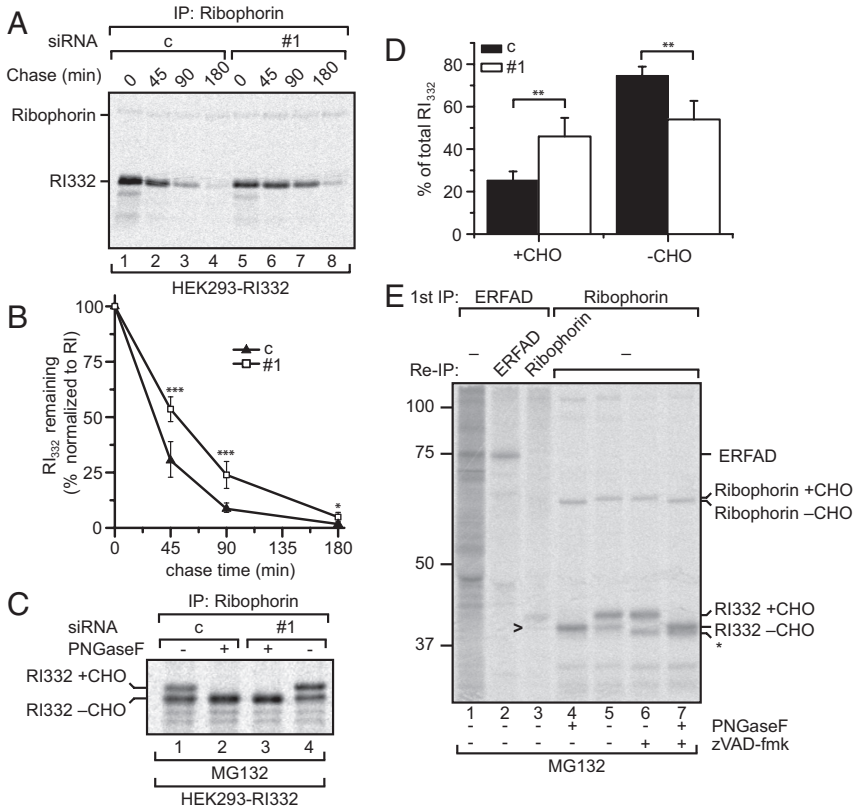

Fig. 3. ERFAD knockdown stabilizes the ERAD model substrate RI_{332}. (*A*) Decay of RI_{332} upon ERFAD knockdown. HEK293 cells stably expressing RI_{332} were transfected with ERFAD siRNA#1 (#1) and nonsilencing control siRNA (c). Seventy-two hours after transfection cells were pulse labeled for 20 min and chased for the indicated times. SDS lysates were subjected to immunoprecipitation with anti-ribophorin. (*B*) Quantification of three independent RI_{332} decay experiments (RI_{332} signal normalized to full length RI). Mean ± SD; ***, $P < 0.005$; *, $P < 0.5$. (*C*) Ratio of the glycosylated ER form of RI_{332} versus the deglycosylated cytosolic form of RI_{332} upon ERFAD knockdown. ERFAD-silenced and control HEK-RI_{332} cells were pulse-labeled for 20 min and chased for 3 h in the presence of MG132. SDS lysates were subjected to immunoprecipitation with anti-ribophorin and half of the eluate was PNGaseF treated. The two glycosylation states of RI_{332} are indicated. (*D*) Quantification of three independent experiments as performed in *C*. **, $P < 0.05$. (*E*) Coimmunoprecipitation of ERFAD and RI_{332}. HEK293-RI_{332} cells were pulse-labeled for 5 h in the presence of MG132. Anti-ERFAD immunoprecipitates were either analyzed directly (lane 1) or reimmunoprecipitated with anti-ERFAD (lane 2) or anti-ribophorin (lane 3). In lanes 4—7, SDS lysates from cells labeled in the presence or absence of zVAD-fmk (+MG132) were immunoprecipitated with anti-ribophorin with or without subsequent PNGaseF digest to allow the assignment of the three different forms of RI_{332} (RI_{332}+CHO, RI_{332}-CHO and *). The arrowhead indicates the minor fraction of deglycosylated RI_{332} (RI_{332}-CHO) interacting with ERFAD. For a contrast-enhanced version, see Fig. S7*A*.

reprecipitating SEL1L (Fig. 2*E*, lanes 3 and 4). When analyzing the precipitate under nonreducing conditions that leave cross-links intact, we found that it appeared as a high molecular weight smear suggesting that ERFAD functions in a larger complex (Fig. 2*I*, lane 8). The identity of the interacting proteins is currently unknown.

ERFAD Knockdown Inhibits the Degradation of RI_{332}. The identification of the three known ERAD components SEL1L, OS-9, and ERdj5 as interaction partners suggested a role of ERFAD in ERAD. For investigations of a potential ERAD function we established siRNA-mediated down-regulation of ERFAD (Fig. S2). Although a slight increase in PERK phosphorylation was observed, ERFAD down-regulation did not considerably induce the unfolded protein response (Fig. S4 *A–C*). Furthermore, it neither influenced significantly the steady-state levels and redox states of selected ER oxidoreductases (PDI, ERp57, and TMX3) or the steady-state level of p97 (Fig. S4 *D–F*), nor did it perturb the oxidative refolding of the disulfide-containing Ig J-chain after DTT washout (Fig. S4*G*). We also investigated the in vivo redox state of ERdj5, and showed it to be almost completely oxidized at steady state (Fig. S4*H*). Unfortunately, the assay did not provide a definite conclusion as to whether the redox state of a single among the four redox-active cysteine pairs in ERdj5 was affected by ERFAD knockdown (see *SI Text* for a discussion). Overall, ERFAD down-regulation did not seem to influence general ER homeostasis and redox conditions.

We next investigated effects of ERFAD down-regulation on model protein degradation. Ribophorin 332 (RI_{332}), a truncated soluble variant of the oligosaccharyl transferase-component ribophorin I (19), is degraded in a SEL1L-dependent manner (5). We therefore tested by pulse–chase analysis the effect of ERFAD knockdown on the stability of RI_{332} in a HEK293 cell line that stably expresses RI_{332} (HEK293-RI_{332}). Immunoprecipitation with anti-ribophorin retrieved both RI_{332} and wild-type ribophorin I. Because the latter remained unaffected by ERFAD knockdown and is a stable protein with a half-life of 25 h (20), it was used to normalize the RI_{332} signal. We observed a significant stabilization of RI_{332} upon ERFAD down-regulation (Fig. 3 *A* and *B*). In contrast, the degradation kinetics of the α-subunit of the T cell receptor complex (TCRα) was not significantly affected by ERFAD knockdown (Fig. S5 *A* and *B*), a result that fits well with the observation that TCRα is only marginally (if at all) influenced by SEL1L down-regulation (5, 21). A similar result was observed for another ERAD substrate, the nonsecreted Ig κ light chain (NS1κLC) (22) (Fig. S5 *C* and *D*). In the same fashion, down-regulation of other ERAD components such as OS-9 and XTP3-B only affected the degradation of certain specific substrates but not of others (8, 23, 24).

ERFAD Knockdown Leads to the Accumulation of the Glycosylated ER Form of RI_{332}. Having established a stabilizing influence of ERFAD down-regulation on RI_{332}, we next investigated the possibility that this effect was due to an accumulation of RI_{332} in the ER lumen. Whereas luminal RI_{332} carries an N-glycan, the cytosolic (retrotranslocated) form becomes deglycosylated by Png1 before degradation by the proteasome (19, 25). This property allows assignment of RI_{332} to the ER or the cytosol. We immunoprecipitated RI_{332} from HEK293-RI_{332} cells that had been pulse-labeled and chased in the presence of the proteasome inhibitor MG132. The result showed that significantly more glycosylated RI_{332} remained upon ERFAD knockdown compared with control conditions (Fig. 3 *C* and *D*). To exclude that MG132 treatment prevented a fraction of RI_{332} from entering the ER and becoming glycosylated, we analyzed HEK293-RI_{332} cells directly after the pulse. Under these conditions, and irrespective of ERFAD knockdown, almost all RI_{332} was present in the glycosylated ER form (Fig. S6), showing that in the above experiment, deglycosylated RI_{332} indeed constituted the retrotranslocated fraction. In summary, our data strongly suggested that RI_{332} is retained in the ER lumen when ERFAD levels are lowered.

ERFAD Interacts with RI_{332}. The results so far indicated that ERFAD, like SEL1L, plays a role in the degradation of RI_{332}. We therefore evaluated whether ERFAD and RI_{332} could be precipitated in the same complex. To this end, we immunoprecipitated ERFAD from extracts of MG132-treated [^{35}S]methionine-labeled HEK293-RI_{332} cells. Indeed, when reimmunoprecipitating RI_{332} we predominantly recovered the glycosylated form of the protein (Fig. 3*E* and Fig. S7*A*, lanes 3 and 3′; the identity of the different RI_{332} forms is discussed in the Fig. S7*A* figure legend). In an equivalent experiment using anti-SEL1L for reimmunoprecipitation, we could show that SEL1L, exactly like ERFAD, mainly coprecipitated glycosylated RI_{332} (Fig. S7*B*). The finding that ERFAD coprecipitates RI_{332}—and not full-length ribophorin (Fig. 3*E*)—further supports the direct involvement of ERFAD in the degradation of this ERAD substrate.

The Level of Polyubiquitinated Proteins Is Decreased upon ERFAD Knockdown. To evaluate the overall role of ERFAD in dislocation of ER proteins targeted for ERAD, we investigated the influence of ERFAD knockdown on the total cellular pool of polyubiquitinated proteins. A fraction of these polyubiquitinated proteins are ERAD substrates that are polyubiquitinated in the cytosol directly after or during extraction from the ER (26). As a positive control we treated cells with MG132, which led to the accumulation of polyubiquitinated proteins (Fig. 4*A*). In contrast, ERFAD knockdown resulted in a clear reduction in the level of polyubiquitinated proteins (Fig. 4 *B* and *C*). The decreased levels of polyubiquitination induced by ERFAD deprivation—very much like the changes in polyubiquitination observed upon knockdown of the ER oxidoreductases PDI and ERp72 (27, 28)—were not accompanied by an induction of the unfolded protein response (Fig. S4).

Conclusions

Our detailed analysis of ERAD model substrate degradation functionally connects the ER-luminal protein ERFAD to ERAD. Moreover, complex formation of ERFAD with SEL1L, OS-9, and ERdj5, and the observed effect of ERFAD knockdown on polyubiquitination provide additional links between ERFAD and the process of ERAD. Because the results were obtained by a variety of experimental techniques (including coprecipitation of endogenous proteins), they are unlikely to reflect indirect effects of ERFAD inactivation or overexpression. Notably, ERFAD down-regulation did not prevent oxidative folding or change general ER redox conditions, and only marginally induced the unfolded protein response. Overall, our results present a coherent set of data that demonstrates a direct role of ERFAD in ERAD.

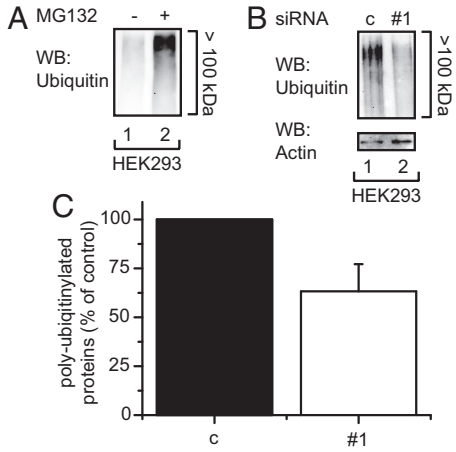

Fig. 4. The knockdown of ERFAD decreases the cellular amount of polyubiquitinated proteins. (*A*) Accumulation of polyubiquitinated proteins upon MG132 treatment. HEK293 cells were either left untreated or treated with MG132, lysates were adjusted by a BCA assay to the same protein concentration and analyzed by Western blotting with anti-ubiquitin. (*B*) Decrease of polyubiquitinated proteins upon ERFAD knockdown. HEK293 cells were transfected with ERFAD siRNA#1 and nonsilencing control siRNA (c). Cells were lysed 72 h after transfection, lysates were adjusted to the same concentration and analyzed by Western blotting with anti-ubiquitin and anti-actin. (*C*) Quantification of three independent experiments performed as described in *B* and plotted as percentage of control, mean ± SD.

We show that the interaction with ERFAD is required for efficient retrotranslocation and degradation of RI_{332}, an established substrate of the SEL1L/Hrd1 ERAD pathway (5). Conversely, we observed no effect of ERFAD knockdown on the degradation of the Hrd1-independent ERAD substrate TCRα (5, 21) or on NS1κLC (Fig. S5), a disulfide-containing ERAD substrate that becomes reduced by an unknown process before retrotranslocation (22). Given the putative redox activity of ERFAD (see below), the identification of RI_{332}, which lacks disulfides, as a substrate for ERFAD may appear unexpected. However, ERFAD need not be restricted to promoting degradation of disulfide-containing ERAD substrates, as illustrated by the finding that the ER oxidoreductase PDI assists the retrotranslocation of Dgpaf, which does not contain disulfides (29).

Our studies show that ERFAD is a flavoprotein. Despite considerable effort, we were unable to purify sufficient amounts of the protein to reliably determine whether it is capable of using NADPH. However, the in silico analysis strongly suggests that ERFAD uses both FAD and NADPH, a unique feature among known ER proteins. Moreover, we show ERFAD to interact with ERdj5 that reduces disulfides in ERAD substrates (13). With FAD and NADPH as redox cofactors, ERFAD should be able to provide the electrons for the reduction of the active-site cysteines in ERdj5. Although we do not have direct evidence that ERFAD is a reductase for ERdj5, this will be an obvious working hypothesis to guide future experiments. Further cell biological and biochemical studies will be aimed at improving mechanistic insight into the function of ERFAD.

Materials and Methods

Primers and Plasmids. The ERFAD cDNA clone IMAGE3873448 (9629-g17) was acquired from the I.M.A.G.E. consortium. The plasmids pcDNA3, pcDNA5-FRT and pOG44 were obtained from Invitrogen. The RI_{332} construct was a gift from N. E. Ivessa, University of Vienna and the NS1 κ LC construct was a gift from L. Hendershot, St. Jude Children's Research Hospital. The following plasmids were constructed as described in *SI Text*: pcDNA3/ERFAD-HA, pcDNA5-FRT/ERFAD-HA, pRSETminiT/His-ERFAD, and pcDNA3/HA-NS1 κ LC (Table S1).

Antibodies. Antibodies against the following proteins and peptide tags were used: actin (Sigma), BiP (Santa Cruz Biotechnology), eIF2α and eIF2α-phosphate (Cellular Signaling), ERdj5 (Abcam), ERp57 (gift from A. Helenius, ETH Zurich), anti-GFP (Invitrogen), HA (12CA5, gift from M. Peter, ETH Zurich and 16B12, Covance), tetra-His (Qiagen), Hsp47 (Stressgen), myc (9E10, Covance), OS-9 (Novus), p97 (30) and p112 (Biomol), PDI (Stressgen), ribophorin (gift from N.E. Ivessa, University of Vienna), SEL1L (gift from H. Ploegh, Whitehead Institute, Cambridge, MA), TMX3 (31), and ubiquitin (Dako). The secondary anti-rabbit and anti-mouse IgG coupled to horseradish peroxidase were obtained from Pierce and the Alexa Fluor 594 anti-mouse IgG from Invitrogen. A polyclonal serum against ERFAD was generated by immunizing rabbits with the full length denatured His-ERFAD protein expressed in *E. coli*. The obtained 1F6 antiserum was affinity purified and used for Western blotting. For immunoprecipitations, the polyclonal anti-peptide serum SG2480 generated by immunizing rabbits with the C-terminal peptide of ERFAD (CGPLAQSVDSNKEEL) was used.

Cell Lines. HEK293-TCRα-GFP cells were a gift of R. Kopito, Stanford University. Stable cell lines were either generated using the Flp-In system from Invitrogen (A11, ERFAD-HA in HEK293-FRT, selected with 0.1 mg/mL hygromycin B) or by calcium phosphate transfection of HEK293 cells with pcDNA3/ERFAD-His-FLAG (3B2B), pcDNA3/RI$_{332}$ (HEK293-RI$_{332}$), pcDNA3/myc-J-chain (HEK293-myc-J-chain), or pcDNA3/HA-NSκLC (HEK293-HA-NSκLC) and subsequent selection with 1 mg/mL geneticin. All cells were cultured in modified Eagle medium alpha (Gibco) supplemented with 10% FCS (LabForce AG). Stable cells were additionally supplemented with the respective antibiotic.

ERFAD-His-FLAG Expression and Purification. ERFAD-His-FLAG was purified from 3B2B cells adapted to suspension growth in spinner flasks. Cells were grown to a density of 1.5×10^6 cells per mL and harvested by centrifugation. The pellet was washed with PBS and resuspended in lysis buffer [TBS (50 mM Tris·HCl, pH 7.5, 150 mM NaCl, containing 1% Triton X-100)]. The cleared lysate was applied onto an M2-FLAG affinity matrix (Sigma). The matrix was washed with 100 bed volumes of lysis buffer followed by TBS and eluted with 0.1 mg/mL FLAG peptide in TBS. ERFAD-containing fractions were pooled, concentrated on a 0.5-mL spin filter (MWCO 30 kDa) and analyzed by SDS/PAGE. Absorption spectra were recorded on a Lambda 35 UV/Vis spectrometer (Perkin-Elmer). The fluorescence of FAD was analyzed by the method of Faeder and Siegel (18) using a LS55 fluorimeter (Perkin-Elmer).

RT-PCR Analysis, Western Blot Analysis, Cell Fractionation, Endoglycosidase H (EndoH) Digests, and Immunofluorescence. Total RNA was isolated (GenElute Total RNA kit, Sigma), the concentration adjusted and mRNA reverse transcribed (Enhanced avian reverse transcriptase kit, Sigma). PCR with primers specific for ERFAD (for: aagaagccaacaccaacc; rev: actcctccaggtactcaaa) and actin (for: ggactcgagcaagagatgg; rev: agcactgtgttggcgtacag) was performed and analyzed on 1% agarose gels. All other methods were performed as described in ref. 31, except for the immunofluorescence on endogenous ERFAD where cells were fixed in methanol for 5 min at −20 °C.

Transfections and siRNA-Mediated Knockdown. Cells were transfected by the calcium phosphate transfection method. For siRNA-mediated knockdown, four siRNAs against ERFAD and a nonsilencing control siRNA (QIAGEN) were generated against the target sequences provided in the *SI Text* and *Materials and Methods*.

MG132, zVAD-fmk, and Cycloheximide Incubations. MG132 (Sigma, 50 mM stock in DMSO) was used at a final concentration of 5 μM in DMEM without FCS. zVAD-fmk (Sigma, 10 mM stock in DMSO) was used at a final concentration of 25 μM in DMEM without FCS. Cycloheximide (Sigma, 10 mg/mL stock in water) was used at a final concentration of 10 μg/mL in MEMα + 10% FCS.

Metabolic Labeling and Immunoprecipitations. Pulse–chase experiments with [^{35}S] Express protein labeling mix (Perkin-Elmer) and immunoprecpitations from cell lysates were performed as described in ref. 32, with the exception that before lysis cells were treated with 20 mM NEM in PBS on ice to block free cysteines. The following IP lysis buffer was used for native immunoprecipitation: 50 mM Hepes/NaOH, pH 7.2, 50 mM NaCl, 125 mM K-acetate, 2 mM $MgCl_2$, 1 mM EDTA, 3% glycerol, and 1% Nonidet P-40. Quantification was performed on phosphorimager scans using the ImageQuant software (GE Healthcare).

DSP Cross-Linking. Cells were washed twice with ice-cold PBS and then incubated with 1 mM DSP (Pierce) in PBS for 20 min. The cross-linking reaction was stopped with 20 mM Tris·HCl, pH 8.0, and 20 mM NEM.

ACKNOWLEDGMENTS. We thank all members of the Ellgaard lab, K. Hendil, and J. Winther for helpful discussions; A.M. Lauridsen, A. Kyburz, C. Ashiono, and M. Nielsen for excellent technical assistance; R. Aebersold for help with mass spectrometry; A. Helenius (ETH Zurich, Zurich), N. E. Ivessa (University of Vienna, Vienna), R. Kopito (Stanford University, Stanford, CA), M. Peter (ETH Zurich, Zurich), L. Hendershot (St. Jude Children's Research Hospital, Memphis, TN), S.T. Christensen (University of Copenhagen, Copenhagen), and H. Ploegh for sharing reagents; and the Institute of Biochemistry, ETH Zurich for support. This work was supported by the Novo Nordisk Foundation, the Danish Natural Science Research Council, and the Novartis Stiftung. J.R. and B.B. are fellows of the Boehringer Ingelheim Fonds and C.A.-H. is a fellow of the Swiss National Science Foundation.

1. Anelli T, Sitia R (2008) Protein quality control in the early secretory pathway. *EMBO J* 27:315–327.
2. Kincaid MM, Cooper AA (2007) ERADicate ER stress or die trying. *Antioxid Redox Signal* 9:2373–2387.
3. Nakatsukasa K, Brodsky JL (2008) The recognition and retrotranslocation of misfolded proteins from the endoplasmic reticulum. *Traffic* 9:861–870.
4. Kikkert M, et al. (2004) Human HRD1 is an E3 ubiquitin ligase involved in degradation of proteins from the endoplasmic reticulum. *J Biol Chem* 279:3525–3534.
5. Mueller B, Lilley BN, Ploegh HL (2006) SEL1L, the homologue of yeast Hrd3p, is involved in protein dislocation from the mammalian ER. *J Cell Biol* 175:261–270.
6. Lilley BN, Ploegh HL (2005) Multiprotein complexes that link dislocation, ubiquitination, and extraction of misfolded proteins from the endoplasmic reticulum membrane. *Proc Natl Acad Sci USA* 102:14296–14301.
7. Mueller B, Klemm EJ, Spooner E, Claessen JH, Ploegh HL (2008) SEL1L nucleates a protein complex required for dislocation of misfolded glycoproteins. *Proc Natl Acad Sci USA* 105:12325–12330.
8. Christianson JC, Shaler TA, Tyler RE, Kopito RR (2008) OS-9 and GRP94 deliver mutant alpha1-antitrypsin to the Hrd1-SEL1L ubiquitin ligase complex for ERAD. *Nat Cell Biol* 10:272–282.
9. Gauss R, Jarosch E, Sommer T, Hirsch C (2006) A complex of Yos9p and the HRD ligase integrates endoplasmic reticulum quality control into the degradation machinery. *Nat Cell Biol* 8:849–854.
10. Carvalho P, Goder V, Rapoport TA (2006) Distinct ubiquitin-ligase complexes define convergent pathways for the degradation of ER proteins. *Cell* 126:361–373.
11. Denic V, Quan EM, Weissman JS (2006) A luminal surveillance complex that selects misfolded glycoproteins for ER-associated degradation. *Cell* 126:349–359.
12. Quan EM, et al. (2008) Defining the glycan destruction signal for endoplasmic reticulum-associated degradation. *Mol Cell* 32:870–877.
13. Ushioda R, et al. (2008) ERdj5 is required as a disulfide reductase for degradation of misfolded proteins in the ER. *Science* 321:569–572.
14. Ye Y, Meyer HH, Rapoport TA (2001) The AAA ATPase Cdc48/p97 and its partners transport proteins from the ER into the cytosol. *Nature* 414:652–656.
15. Rabinovich E, Kerem A, Frohlich KU, Diamant N, Bar-Nun S (2002) AAA-ATPase p97/Cdc48p, a cytosolic chaperone required for endoplasmic reticulum-associated protein degradation. *Mol Cell Biol* 22:626–634.
16. Suzuki T, Park H, Hollingsworth NM, Sternglanz R, Lennarz WJ (2000) PNG1, a yeast gene encoding a highly conserved peptide:N-glycanase. *J Cell Biol* 149:1039–1052.
17. Richly H, et al. (2005) A series of ubiquitin binding factors connects CDC48/p97 to substrate multiubiquitylation and proteasomal targeting. *Cell* 120:73–84.
18. Faeder EJ, Siegel LM (1973) A rapid micromethod for determination of FMN and FAD in mixtures. *Anal Biochem* 53:332–336.
19. de Virgilio M, Weninger H, Ivessa NE (1998) Ubiquitination is required for the retrotranslocation of a short-lived luminal endoplasmic reticulum glycoprotein to the cytosol for degradation by the proteasome. *J Biol Chem* 273:9734–9743.
20. Tsao YS, Ivessa NE, Adesnik M, Sabatini DD, Kreibich G (1992) Carboxy terminally truncated forms of ribophorin I are degraded in pre-Golgi compartments by a calcium-dependent process. *J Cell Biol* 116:57–67.
21. Cattaneo M, et al. (2008) SEL1L and HRD1 are involved in the degradation of unassembled secretory Ig-micro chains. *J Cell Physiol* 215:794–802.
22. Okuda-Shimizu Y, Hendershot LM (2007) Characterization of an ERAD pathway for nonglycosylated BiP substrates, which require Herp. *Mol Cell* 28:544–554.
23. Bernasconi R, Pertel T, Luban J, Molinari M (2008) A dual task for the Xbp1-responsive OS-9 variants in the mammalian endoplasmic reticulum: Inhibiting secretion of misfolded protein conformers and enhancing their disposal. *J Biol Chem* 283:16446–16454.
24. Hosokawa N, et al. (2008) Human XTP3-B forms an endoplasmic reticulum quality control scaffold with the HRD1-SEL1L ubiquitin ligase complex and BiP. *J Biol Chem* 283:20914–20924.
25. Kitzmuller C, et al. (2003) Processing of N-linked glycans during endoplasmic-reticulum-associated degradation of a short-lived variant of ribophorin I. *Biochem J* 376:687–696.
26. Elkabetz Y, Shapira I, Rabinovich E, Bar-Nun S (2004) Distinct steps in dislocation of luminal endoplasmic reticulum-associated degradation substrates: Roles of endoplamic reticulum-bound p97/Cdc48p and proteasome. *J Biol Chem* 279:3980–3989.
27. Forster ML, et al. (2006) Protein disulfide isomerase-like proteins play opposing roles during retrotranslocation. *J Cell Biol* 173:853–859.
28. Schelhaas M, et al. (2007) Simian Virus 40 depends on ER protein folding and quality control factors for entry into host cells. *Cell* 131:516–529.
29. Wahlman J, et al. (2007) Real-time fluorescence detection of ERAD substrate retrotranslocation in a mammalian in vitro system. *Cell* 129:943–955.
30. Hartmann-Petersen R, et al. (2004) The Ubx2 and Ubx3 cofactors direct Cdc48 activity to proteolytic and nonproteolytic ubiquitin-dependent processes. *Curr Biol* 14:824–828.
31. Haugstetter J, Blicher T, Ellgaard L (2005) Identification and characterization of a novel thioredoxin-related transmembrane protein of the endoplasmic reticulum. *J Biol Chem* 280:8371–8380.
32. Appenzeller-Herzog C, et al. (2005) Carbohydrate- and conformation-dependent cargo capture for ER-exit. *Mol Biol Cell* 16:1258–1267.